Human Genomics

RESEARCH

Open Access

Genetic landscape and ocular biometric correlations in microspherophakia: insights from a comprehensive patient cohort

Yan Liu[1,2,3†], Yang Sun[1,2,3†], Qiuyi Huo[1,2,3], Linghao Song[1,2,3], Xinyue Wang[1,2,3], Xin Shen[1,2,3], Ye Zhao[4], Tianhui Chen[1,2,3*†] and Yongxiang Jiang[1,2,3*†]

Abstract

Aims The aim of this study is to elucidate the genetic landscape of microspherophakia (MSP) and describe the genotype-phenotype correlation of MSP. Additionally, the study seeks to enhance the understanding of the pathogenic mechanisms of MSP through the discovery of novel loci.

Methods Patients diagnosed with MSP at the Eye and ENT Hospital of Fudan University, Shanghai, were included in the study and all underwent panel-based next-generation sequencing and bioinformatics analysis. Comprehensive ophthalmologic evaluations were conducted for each participant.

Results Our analysis encompassed 118 eyes from 59 patients with MSP, revealing 13 gene variations linked to the condition. Notably, *FBN1* mutations were identified in 31 patients (52.5%), highlighting its higher prevalence. Among the genetic variations discovered, 28 represented novel mutations. Statistical analysis unveiled significant associations between specific gene mutations and ocular biometric parameters: axial length (AL, $p=0.011$), Z-score axial length (Z-AL, $p<0.001$), white-to-white (WTW, $p=0.009$), Z-score white-to-white ($p=0.012$), mean keratometry ($p<0.001$), astigmatism (AST, $p=0.021$), anterior chamber depth (ACD, $p=0.003$), lens thickness (LT, $p=0.012$) and central endothelial cell count/mm2 ($p=0.005$). Patients with *FBN1* mutations had the longest AL, while those with *CBS* mutations showed significantly wilder WTW measurements. Patients with *ADAMTS17* mutations presented with increased LT and decreased WTW, *ADAMTSL4* mutations were linked to the greater Km and AST. Patients with *LTBP* mutations exhibited the largest WTW, and *ASPH* mutations was associated with the shortest AL but thick LT. Additionally, there was a relationship among gene mutations, diagnostic age and ocular biometric parameters.

Conclusion The study demonstrates that MSP is associated with a diverse range of genetic mutations, with FBN1 being the most common. Novel mutations were identified, and significant correlations were found between specific genetic variations and ocular biometric parameters. These results provide new insights into the genetic

†Yan Liu and Yang Sun contributed equally as co-first authors.

*Correspondence:
Tianhui Chen
chentianhui97@163.com
Yongxiang Jiang
yongxiang_jiang@163.com

Full list of author information is available at the end of the article

underpinnings of MSP and its clinical characteristics, advancing our understanding of the condition's pathogenic mechanisms.

Keywords Microspherophakia, Genotype-phenotype correlation, Genetic landscape, Ocular biometric parameters

Introduction

Microspherophakia (MSP) is a rare congenital ocular disorder that significantly alters lens shape, characterized by an increased anteroposterior distance and a reduced equatorial diameter [1]. It has been reported that the incidence of MSP exceeds 1 per 100,000 individuals, with a study conducted in India reporting a prevalence rate as high as 1.5% among children [2]. MSP frequently presents with a range of ocular complications, including high lenticular myopia, premature loss of accommodative ability, and secondary glaucoma [1, 3]. The incidence of MSP in ectopia lentis (EL) was 10.4% [4]. Moreover, the incidence of angle-closure glaucoma in MSP patients has been documented to range from 44.4–51% [1, 5].

MSP is commonly observed as a phenotype in various genetic syndromes, such as Marfan syndrome (MFS), Weil-Marchesani syndrome (WMS), Homocysteinuria, and Axenfield-Rieger syndrome, among others [6]. Consequently, MSP encompasses a broad spectrum of pathogenic genes. Currently reported pathogenic genes for MSP include *LTBP2*, *FBN1*, *ADAMTS17*, *ADAMTSL4* and others [7–9]. Different mutations affect the growth and function of ciliary zonular through different pathways, resulting in varied clinical features and complications of MSP. For instance, mutations in *LTBP2* can lead to MSP and typical inferior or anterior dislocation. Conversely, most EL occur in an upward direction with mutations in *FBN1* [10, 11]. Pupillary block glaucoma leading to angle closure is believed to be common in the mutations of *LTBP2* and *CBS* [12, 13].

In summary, the genetic diversity underlying MSP presents significant challenges in diagnosis, emphasizing the importance of detailed morphological assessments and genetic analyses to achieve accurate identification and understanding of this condition. Currently, there is a lack of a comprehensive and extensive research on MSP, most of which are limited to small case reports. Particularly, studies of phenotypic differences among various gene mutations are limited.

Thus, we conducted a study involving 59 MSP probands, the largest known cohort to our knowledge. The aim of this study was to summarize the pathogenic genes of MSP and construct a comprehensive landscape of its genetic underpinnings. Furthermore, we intended to analyze the relationship between specific genotypes and phenotypes, hoping that this study would provide novel insights into the pathogenesis of MSP and bridge the gap between molecular findings and clinical manifestations.

Methods

Patient eligibility

A total of 59 probands diagnosed with MSP were included in this study, spanning the period from January 2016 to December 2023. These patients were identified during their visits to the Eye and ENT Hospital of Fudan University in Shanghai, China. Ethical approval for this study was obtained from the institutional review board, which recognized it as an extension of our previously registered randomized controlled trial (ChiCTR2000039132), conducted in accordance with the principles outlined in the Declaration of Helsinki. Informed consent was obtained from all participants, including consent for the protection of their personal data. The inclusion criteria were as follows: (1) a confirmed diagnosis of MSP; (2) availability of comprehensive clinical data and family histories. MSP diagnosis was based on a combination of characteristic morphological features and genetic analysis. Diagnostic criteria included: bilateral involvement; lenticular myopia; visibility of the equatorial edge of the lens under slit-lamp or operating microscope after mydriasis; sparse and lax zonular fibers observed via ultrasound biomicroscopy; and lens dislocation detectable in the supine position [14]. MSP is typically a genetic disorder and can occur in association with conditions such as Weill-Marchesani syndrome, Marfan syndrome, Alport syndrome, and Klinefelter syndrome [1]. Patients with the following features were excluded: (1) coexistence of pathogenic mutations of other ocular diseases; (2) history of trauma in either of the eyes; (3) comorbidities including endophthalmitis, end-stage glaucoma, and atrophy of eyeball. To minimize potential selection bias stemming from familial clustering, only probands from pedigrees were enrolled. The age at which clinical features were first observed was documented for each participant.

Ophthalmic examinations

Comprehensive ophthalmic assessments were conducted for all participants conducted by board-certified ophthalmologists. The examinations comprised slit-lamp biomicroscopy, corneal pachymetry, spectral-domain optical coherence tomography, and topography analyses using the Pentacam HR system (Oculus, Wetzlar, Germany). The diagnosis of MSP was established via slit-lamp examination performed with complete pupillary dilation, revealing increased lens thickness and reduced equatorial diameter. Axial length (AL) measurements were obtained using the IOLMaster 700 (Oculus Inc., Wetzlar, Germany), which utilizes a rotating Scheimpflug camera.

Intraocular pressure (IOP) was assessed with a non-contact tonometer (CT-80, Topcon, Oakland, USA). Ultrasound biomicroscopy (UBM) was utilized to visualize the anterior chamber angle and anterior segment structures. The severity of EL was graded according to the classification method established by Chen et al. [4].

Genetic screening

Genetic screening was performed utilizing a panel-based Next-Generation Sequencing (NGS) methodology, in accordance with established protocols outlined in our previous publications [15]. Genomic DNA extraction from peripheral blood samples was carried out using the CWE2100 Blood DNA Kit (Auto Plate, CWBIO, #CW2526). The pathogenicity of the identified variants was assessed using several bioinformatics tools [15]. The novelty of the variants was assessed using the Human Gene Mutation Database (HGMD). The potential impacts of newly discovered missense mutations on protein function were predicted using MutationTaster (http://mutationtaster.org), SIFT (http://sift.jcvi.org), and PolyPhen-2 (http://genetics.bwh.harvard.edu/pph2/). The novel variants were classified according to the ACMG criteria as pathogenic, likely pathogenic, or of uncertain clinical significance (VUS). Protein predict model (Swiss model, AlphaFold2) was employed to display the protein structures of newly identified missense mutations. By predicting potential structural changes, these models illustrate how the mutations may impact the protein's structure and function, aiding in the understanding of their pathogenicity and role in the disease mechanism.

Statistical analyses

All data analyses were executed with SPSS version 20.0 (IBM Corp., Armonk, NY, USA). We calculated the Z-scores of AL and WTW (white-to-white) using the following formula: Z-score = (measured parameter–normative parameter) / normative standard deviation, which allows for age adjustment [16]. Continuous variables are presented as means ± standard deviation (SD). The normality of continuous data was assessed using the Kolmogorov-Smirnov test. Two-group comparisons were performed using the t-test for normally distributed data or the Mann-Whitney U test for non-normally distributed data. Multigroup comparisons were conducted using one-way analysis of variance (ANOVA) for normally distributed data or the Kruskal-Wallis test for non-normally distributed data. Categorical variables were summarized as frequencies and percentages, and comparisons were made using the $\chi 2$ test or Fisher's exact test as appropriate. Statistical significance was defined as $p < 0.05$ for all analyses.

Results

Cohort characteristics

Table 1 presents the demographic characteristics and ocular biometric parameters of the patients comprising this cohort. The cohort comprised 59 individuals diagnosed with MSP, including 30 females and 29 males. Average patient age was 16.08 ± 16.09 years. In the analysis of 118 eyes examined, 96 (81.36%) exhibited EL, categorized as mild in 45 eyes, moderate in 6 eyes, and severe in 35 eyes. Six individuals were diagnosed with glaucoma, with an average IOP of 15.43 ± 5.42 mmHg. 16.8% of the patients exhibited cataracts earlier than expected. Additionally, nearly all (94.9%) of the patients were diagnosed with bilateral myopia, with 15.3% of patients even developing amblyopia. After adjusting for age, the Z-score for AL (Z-AL) was 1.85 ± 3.23 mm, and for WTW (Z-WTW) was 0.39 ± 1.60 mm. Notably, the mean lens thickness (LT) in MSP patients was 4.63 ± 0.91 mm.

Genetic variants spectrum

In our cohort, 13 distinct gene mutations were identified, the most prevalent mutation was found in the *FBN1* gene, detected in 31 (52.5%) of the probands. Subsequently, mutations were observed in *ADAMTS17* (5 probands), *CBS* (5 probands), *LTBP2* (4 probands), *ADAMTSL4* (3 probands), *ASPH* (2 probands), *COL18A1* (1 proband), *COL5A2* (1 proband), *COL4A5* (1 proband), *SLC16A1* (1 proband), *CNGB3* (1 proband), *PTCH1* (1 proband), and *SUOX* (1 proband) (Fig. 1A). Subsequent to our genetic interrogation, 28 mutation sites were not cataloged in public gene databases, with 13 of these sites being previously documented (Table 2). Within this set, 10 novel mutation sites were identified within the *FBN1* gene, with 8 of these predicted to be pathogenic or likely pathogenic mutations, and 6 were intron mutations. *LTBP2* mutations were found to be autosomal recessive, with four newly emerging mutation sites classified as VUS. Among the seven newly emerging *CBS* mutation sites, four were classified as likely pathogenic or pathogenic mutations, while three were categorized as VUS. The mutation site map illustrated in Fig. 1B reveals a spatial distribution pattern, with *FBN1* mutations predominantly localized in the N-terminal and middle regions, *ADAMTSL4* mutations primarily clustered in the thrombospondin type 1 (TSP1) region of the C-terminal, and *CBS* gene mutations concentrated in the N-terminal region. Detailed mutation information is provided in Supplementary Table 1.

Analysis encompassed thirteen genes, with four patients showing no detectable mutations. Baseline characteristics of six genes with high mutation frequencies in this cohort are presented in Table 3, while information on the remaining seven genes is provided in Supplementary Table 1, as their lower mutation frequencies were insufficient for statistical analysis. Significant differences

Table 1 The spectrum of new mutations detected in this study

Gene	Heredity	Nucleotide	Amino Acid Change	Feature	Effect	ACMG
FBN1	AD	c.3244G > T	p.G1082C	New	Missense	Pathogenic
FBN1	AD	c.4211_4336dup	-	New*	Stop gain	Pathogenic
FBN1	AD	c.2419 + 1G > T	-	New	Splice variation	Likely Pathogenic
FBN1	AD	c.2168-1G > C	-	New*	Splice variation	Likely Pathogenic
FBN1	AD	c.5719 + 5G > A	-	New*	Frameshift insertion	Likely Pathogenic
FBN1	AD	c.4943_5422del	-	New*	Frameshift deletion	Pathogenic
FBN1	AD	c.3476G > T	p.C1159F	New	Missense	Pathogenic
FBN1	AD	c.1961_2113del	-	New	Frameshift deletion	Pathogenic
FBN1	AD	c.2659T > C	p.C887R	New	Missense	VUS
FBN1	AD	c.731G > T	p.C244F	New	Missense	VUS
LTBP2	AR	c.643G > A	p.G215R	New*	Missense	VUS
LTBP2	AR	c.3854G > A	p.C1285Y	New	Missense	VUS
LTBP2	AR	c.5392G > A	p.G1798S	New*	Missense	VUS
LTBP2	AR	c.2741delA	p.Y914Sfs*95	New*	Frameshift deletion	VUS
ADAMTS17	AR	c.2181_2182insGAAG	p.I728Efs*52	New	Frameshift insertion	Likely Pathogenic
ADAMTS17	AR	c.203_219del	p.P68Rfs*119	New	Frameshift deletion	Pathogenic
ADAMTSL4	AR	c.2488dupC	p.S832Qfs*5	New*	Frameshift insertion	Likely Pathogenic
COL4A5	AD	c.3940 C > T	p.P1314S	New*	Missense	VUS
SLC16A12	AD	c.977del	p.G326Efs*12	New	Frameshift deletion	Pathogenic
ASPH	AR	c.1126 C > T	p.R376X	New	Nonsense	Pathogenic
ASPH	AR	c.2075G > A	p.G692D	New	Missense	VUS
CBS	AR	c.407T > C	p.L136P	New*	Missense	Likely Pathogenic
CBS	AR	c.111del	p.A38Pfs*44	New	Frameshift deletion	Likely Pathogenic
CBS	AR	c.188 C > T	p.S63F	New	Missense	VUS
CBS	AR	c.457G > C	p.G153R	New*	Missense	VUS
CBS	AR	c.487_495del	p.Y163_C165del	New*	Frameshift deletion	VUS
CBS	AR	c.517_531del	p.M173_K177del	New*	In-frame deletion	Likely Pathogenic
CBS	AR	c.19dup	p.Q7Pfs*30	New	Frameshift deletion	Pathogenic

ACMG = American College of Medical Genetics and Genomics, AD = Autosomal dominant, AR = Autosomal recessive, VUS = variants of unknown significance. *New = has been reported by our group, New = has not been reported

in age at diagnosis were observed among patients with mutations in *FBN1*, *CBS*, *ADAMTS17*, *ADAMTSL4*, *LTBP2*, and *ASPH*, with patients harboring *ADAMTS17* mutations tend to be older, while those with mutations in the remaining genes were predominantly under 20 years of age. Varying degrees of EL were observed among patients with *FBN1* and *CBS* mutations, while patients with other mutations predominantly exhibited mild EL ($p < 0.001$). Glaucoma was associated with mutations in both *COL4A5* and *COL5A2*. Patients with *ADAMTS17* mutations exhibited a glaucoma incidence of 20.0%, with a mean IOP of 20.70 ± 7.03 mmHg. Significant variations in IOP were observed among patients with mutations in six genes ($p < 0.001$). Comparatively, patients with *FBN1* mutations demonstrated longer AL and deeper anterior chamber depth (ACD). Patients with *ASPH* mutations exhibited shorter AL, shallower ACD, and reduced corneal endothelial cell counts compared to their counterparts. The ACD of patients with *COL4A5* mutations was shallow, averaging 1.50 ± 0.71 mm. Patients with *ADAMTS17* mutations displayed a smaller WTW, whereas those with *LTBP2* mutations had a larger WTW ($p = 0.009$). Patients with *ADAMTS17* mutations presented with thicker lens thickness (LT) measuring 5.45 ± 0.40 mm ($p = 0.012$). Patients with *ADAMTSL4* mutations exhibited the greatest mean keratometry (Km) values and corneal astigmatism (AST), while those with *FBN1* mutations demonstrated the lowest Km and AST (Table 3).

Figure 2 presents characteristic photographs of the anterior segment of patients along with relevant gene mutation information. In Fig. 2A, an *FBN1* mutation (c.2638G > A, p.G880S) is depicted in a 22-year-old male patient. This mutation has been conclusively deemed pathogenic and is suspected to be *de novo* or due to germline mosaicism, as it was not detected in his parents. Notably, both lenses of the patient exhibited superior nasal subluxation. Figure 2B illustrates a female patient with an *ADAMTS17* mutation (c.2292G > C, p.L764F) diagnosed at the age of 64 years. This homozygous mutation is a missense mutation. Subluxation of the inferior lenses with nuclear opacities was observed in both eyes of the patient. In Fig. 2C, a female patient with *COL5A2* mutation (c.2884 C > T, p.P962T) diagnosed at the age

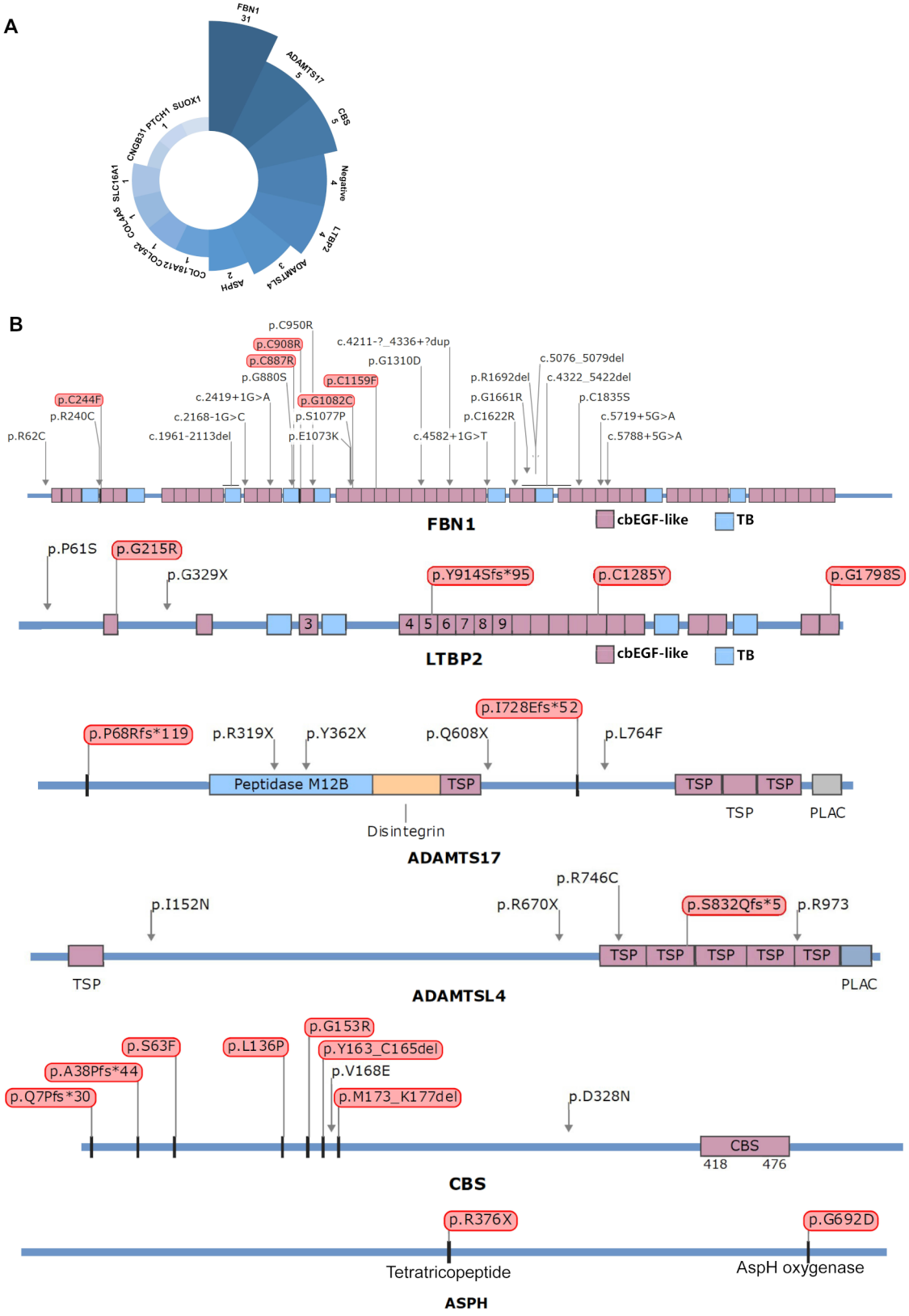

Fig. 1 Distribution of gene mutations associated with microspherophakia (MSP) in 118 probands, with 8 (6.78%) did not detect any mutation. (**A**) The contribution of MSP associated genes in this study. (**B**) The distribution and domain of *FBN1*, *LTBP2*, *ADAMTS17*, *ADAMTSL4*, *CBS* and *ASPH* mutations in our cohort. Novel mutations are highlighted in red

Table 2 Baseline characteristics for patients in this cohort

		Total
Patients		
	Number, *n* (%)	59 (100.0%)
	Sex (female/male)	30/29
	Age, years	16.08 ± 16.09
	Glaucoma, *n* (%)	6 (10.2%)
	Cataract, *n* (%)	10 (16.8%)
	Retinopathy, *n* (%)	2 (3.4%)
	Myopia, *n* (%)	56 (94.9%)
	Amblyopia, *n* (%)	9 (15.3%)
Eyes		118
	Right/left	59/59
	IOP	15.43 ± 5.42
	IOP degree, *n* (%)	
	< 10	10 (8.5%)
	10, 21	92 (78.0%)
	> 21	12 (10.2%)
	AL (mm)	24.79 ± 2.89
	Z-AL	1.85 ± 3.23
	WTW (mm)	12.15 ± 0.60
	Z-WTW	0.39 ± 1.60
	Km (D)	41.40 ± 2.44
	AST (D)	1.78 ± 1.41
	CCT (μm)	535 ± 56
	ACD (mm)	2.83 ± 0.79
	LT (mm)	4.63 ± 0.91
	Central ECC (cells/mm2)	2992 ± 476

ACD = anterior chamber depth; AL = axial length; AST = corneal astigmatism; CCT = central corneal thickness; ECC = endothelial cell count; EL = ectopia lentis; Km = mean keratometry; LT = lens thickness; WTW = white-to-white measurement

of 30 is presented. Pathogenicity prediction for this missense mutation suggested a likely benign outcome. No dislocation of lens was observed, and UBM examination revealed MSP in both eyes, along with protrusion of the anterior and posterior surfaces of the lens, shallow anterior chambers, and secondary angle-closure glaucoma. The location and structural illustration of four novel missense mutations in the 3D protein structure are shown in Fig. 3.

Genotype-phenotype correlation analyses

Analysis of diagnostic age across all patients revealed that *FBN1* mutations predominantly presented earlier than 30 years of age, characterized by a significant prevalence of diagnosis occurring before 10 years of age. Patients harboring *CBS*, *ADAMTSL4*, and *LTBP2* mutations were also diagnosed at 30 years of age or earlier (Fig. 4A). In contrast, MSP patients with *ADAMTS17* mutations were diagnosed later than 30 years of age. In particularly, a case carrying *ADAMTS17* mutations was not diagnosed until the age of 64 years. Figure 4B illustrates that the mean LT among patients with six gene mutations surpassed 4 mm, with those carrying *ASPH* and *ADAMTS17* mutations displaying the highest LT. Importantly, the difference in LT was found to be statistically significant among patients with these six mutations. MSP represent developmental genetic disorders, exhibiting distinct trends and absolute values in ocular biometric parameters with increasing age (Fig. 4C).

Discussion

MSP is defined by a distinctive spherical lens instead of the typical flat oval shape [17]. Being a crucial refractive medium within the eye, alterations in the morphology of the lens significantly impact normal visual quality. MSP, being a hereditary disorder, frequently manifests alongside various complications, encompassing ocular issues such as megalocornea, high lens myopia and angle-closure glaucoma, as well as many systemic manifestations like aortic dilatation and skeletal abnormalities [1, 17–19]. These complications profoundly diminish the quality of life for affected individuals.

In this study, we have included the largest number of probands with confirmed MSP to our knowledge. Our purpose was to establish a comprehensive landscape of pathogenic genes associated with MSP while describing the clinical phenotype characteristics. A total of 28 novel MSP mutations were unveiled, with 15 of these mutations being previously undocumented. This result serves to greatly broaden the spectrum of gene mutations associated with MSP, thereby enhancing our understanding of the genetic background of MSP [13].

Regarding the pathological mechanism of MSP, some scholars believe that it arises from the disruption of normal lens development [1]. These anomalies are considered secondary to nutritional deficiencies resulting from defects in the vascular membrane of the lens [1]. Such aberrations typically manifest between the fifth to sixth months of embryonic life, a period during which the lens assumes a spherical shape [20]. An alternative viewpoint suggests that MSP may arise from a deficiency in tension within the rudimentary ciliary zonule, which impede lens development and thus maintaining its spherical configuration [21]. With the increasing understanding of MSP, the latter perspective gains further support. Consistent with the findings of this study, examination of 59 probands revealed the presence of 13 pathogenic genes, all of which affect collagen fibers of the ciliary zonule.

The fibrillin-1 encoded by *FBN1* gene is the main component of ciliary zonule, and its mutation is widely acknowledged as the primary cause of Marfan syndrome (MFS) [15]. Moreover, 11% of patients with *FBN1* mutations also exhibit MSP [22]. The impact of *FBN1* mutations on MSP was both remarkable and prevalent. In this study, MSP patients with *FBN1* mutations had the longest AL, which was also longer than MFS patients in other studies, yet exhibited milder anterior segment

Table 3 Baseline characteristics for patients in six different groups

	FBN1	CBS	ADAMTS17	ADAMTSL4	LTBP2	ASPH	*P*
Patients							
Number, *n* (%)	31	5	5	3	4	2	-
Sex (female/male)	14: 17	3: 2	5: 0	2: 1	2: 2	0: 2	0.955
Age, years	12.76 ± 14.64	9.40 ± 7.23	44.20 ± 12.16	13.67 ± 11.26	12.00 ± 7.00	5	**< 0.001**
Glaucoma, *n* (%)	1 (3.2%)	0 (0.0%)	1 (20.0%)	0 (0.0%)	0 (0.0%)	0 (0.0%)	0.968
Eyes							
IOP, *n* (%)	13.52 ± 5.95	13.20 ± 2.53	20.70 ± 7.03	16.50 ± 1.87	19.14 ± 5.82	13.50 ± 1.73	**< 0.001**
< 10	9 (90.0%)	1 (10.0%)	0 (0.0%)	0 (0.0%)	0 (0.0%)	0 (0.0%)	**0.044**
10, 21	45 (58.4%)	9 (11.7%)	8 (10.4%)	6 (7.8%)	5 (6.5%)	4 (5.2%)	
> 21	4 (50.0%)	0 (0.0%)	2 (25.0%)	0 (0.0%)	2 (25.0%)	0 (0.0%)	
AL (mm)	25.63 ± 3.03	24.13 ± 3.25	23.79 ± 2.15	24.04 ± 2.51	24.15 ± 2.70	20.94 ± 0.54	**0.011**
Z-AL	3.11 ± 3.32	1.25 ± 2.52	-0.72 ± 2.40	0.50 ± 1.70	0.85 ± 2.06	-2.02 ± 0.79	**< 0.001**
WTW (mm)	12.18 ± 0.58	12.07 ± 0.16	11.7 ± 0.61	12.18 ± 0.25	12.78 ± 0.74	12.58 ± 0.61	**0.009**
Z-WTW	0.53 ± 1.51	0.39 ± 0.89	-0.76 ± 1.52	0.30 ± 0.77	2.26 ± 1.70	1.51 ± 1.60	**0.012**
Km (D)	39.91 ± 1.98	41.1 ± 0.61	44.44 ± 1.13	44.80 ± 1.54	43.34 ± 0.91	43.83 ± 0.34	**< 0.001**
AST (D)	1.64 ± 1.39	2.97 ± 2.19	2.51 ± 2.01	3.06 ± 0.15	1.90 ± 1.14	2.48 ± 1.11	**0.021**
CCT (μm)	518 ± 42	568 ± 71	534 ± 45	551 ± 33	547 ± 83	480 ± 11	0.122
ACD (mm)	3.09 ± 0.83	2.75 ± 0.57	2.52 ± 0.31	2.79 ± 0.29	2.96 ± 0.81	1.64 ± 0.14	**0.003**
LT (mm)	4.51 ± 1.120	4.72 ± 0.39	5.45 ± 0.40	4.17 ± 0.80	4.52 ± 0.46	4.46 ± 0.09	**0.012**
Central ECC (cells/mm2)	3141 ± 511	2983 ± 449	2564 ± 270	3128 ± 178	2847 ± 247	2714 ± 17	**0.005**

ACD = anterior chamber depth; AL = axial length; AST = corneal astigmatism; CCT = central corneal thickness; ECC = endothelial cell count; Km = mean keratometry; LT = lens thickness; WTW = white-to-white measurement

abnormalities [4]. Our findings reveal that *FBN1* mutation sites in MSP patients were predominantly occur in the middle region (exons 22–42), particularly within the neonatal region (exons 24–32), rather than the N-terminal region typically implicated in MFS [22, 23]. Putnam et al. suggested that in neonatal and severe MFS patients, mutations in the FBN1 gene tend to cluster in exons 24–32, which is therefore referred to as the neonatal region [23]. This suggests potential unique mechanisms underlying axial elongation and manifestation of MSP conferred by *FBN1* mutations in this middle region. Therefore, MSP patients should be alert to the location of *FBN1* mutation, particularly if it is within the neonatal region, as mutations in this region have been shown to be associated with more severe phenotypes of MFS, especially systemic complications [21, 22]. As a result, regular screenings for systemic issues, such as cardiovascular abnormalities, are recommended for patients with *FBN1* mutations presenting with MSP [24, 25]. Meanwhile, given the increased severity of EL and more severe ciliary zonule lesions in this subgroup, adequate preparation before surgery is necessary.

In addition to *FBN1*, we have identified multiple genes associated with the onset of MSP, including *ASPH*, *PTCH1*, and *ADAMTS17*. These genes can impact MSP through diverse mechanisms, from the ciliary zonule's developmental process to its assembly and precise localization within the eye. The formation of the ciliary zonule originates from NPCEC (non-pigmented ciliary epithelial cells), extending and positioning on the posterior surface of the lens capsule [26]. The emergence of three distinct groups of ciliary zonule is driven by the different growth rates and developmental directions between the ciliary body and the lens. Genes interacting with any stage of this complex process could potentially lead to MSP.

For example, LTBP2 acts as a bridge structure between microfibrils, vital for the stable assembly of microfibril bundles, providing mechanical strength to ciliary zonules [13, 27, 28]. *ADAMTS17* encoding secreted metalloproteinases that are instrumental in the secretion of fibrillin-1 and therefore plays pivotal roles in the assembly and maturation of microfibril [29–33]. *ASPH* gene is involved in the activation of fibrillin-1, with it's encode aspartic acid/asparagine-β-hydroxylase responsible for post-transcriptional hydroxylation of EGF domain containing proteins, namely FBN1 and LTBP2 [34, 35]. ADAMTSL4 plays an important role in stabilizing ciliary zonule to the lens capsule. Despite its limited presence, being a minor component in the ciliary zonule, its synthesis primarily occurs during the embryonic development of the eye, with expression sharply decreasing after birth, resulting in an early onset of the disease in patients [36]. Previous studies have indicated that the direction of EL in patients with *ADAMTSL4* mutations is inferior-temporal direction, as opposed to the superior dislocation commonly observed in patients with *FBN1* mutations [37, 38]. *PTCH1* also effects the synthesis of fibrillin-1, with its mutations inhibiting the transcription of genes encoding members of the TGF-β and Wnt signaling protein families.

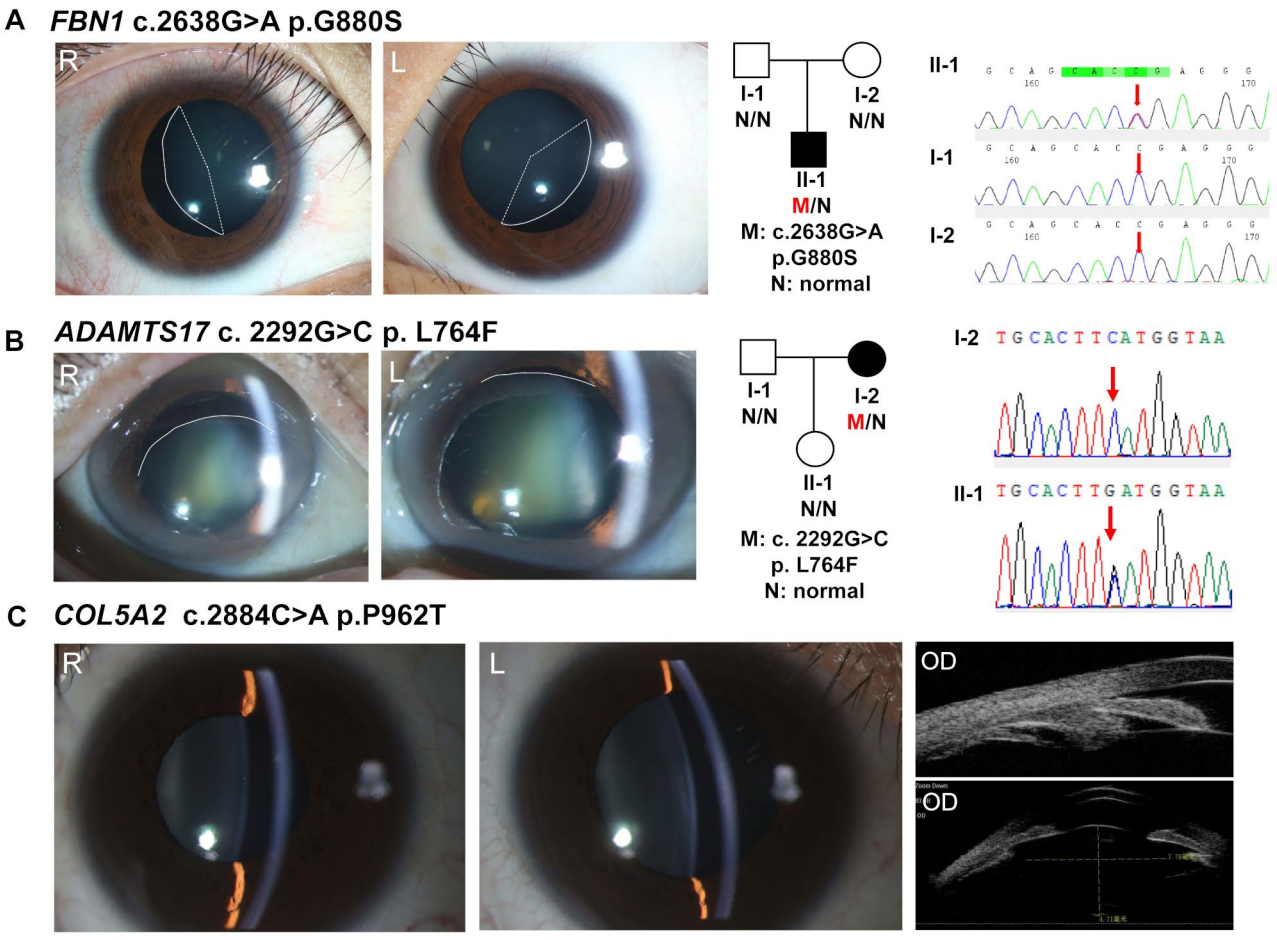

Fig. 2 Representative photographs of microspherophakia (MSP) patients and their pedigree chart. (**A**) A 22-year-old male patient carries FBN1 mutation (c.2638G > A p.G880S), with bilateral moderate lens dislocated to the quadrant above the nose. The mutation was not detected in the patient's parents, suggesting a de novo mutation or germline mosaicism. (**B**) A 64-year-old female patient carries ADAMTS17 mutation (c.2292G > C p.L764F), with bilateral cataracts and mild lens dislocated to the lower quadrant. The white curves from A to B represent the boundaries of the lens, with the white dashed lines indicating links between the boundary intersections and the center. The red arrows point to the mutation sites. (**C**) A 30-year-old female patient's slit lamp photo and ophthalmic UBM report. The patient carries COL5A2 mutation (c.2884C > A p.P962T), presenting with bilateral angle-closure glaucoma. The UBM reveals that the patient's right eye has a shallow anterior chamber, iris bombe, pronounced anterior and posterior lens surfaces, and increased thickness. MSP = microspherophakia, R/L = right/left, OD = right eye, M = mutation, N = normal

Given that these genes are not only expressed in NPCEC but also in other eye cells such as the retina and cornea, attention must be paid to other ocular complications beyond MSP. For instance, mutations in *ADAMTSL4* are frequently associated with glaucoma, ectopia pupil, cataract, and retinal detachment [39]. Like ADAMTS17, AMDATSL4 belongs to the larger superfamily of ADAMTS proteases and ADAMTS-like proteins [40, 41]. The presence of *ADAMTS17* mutations has been shown to be associated with retinopathy in animal models. We observed that patients with *LTBP2* mutations have significantly higher IOP compared to those with other gene mutations, although the exact pathogenic mechanism between *LTBP2* mutations and glaucoma remains unclear [13]. Mutations in *LTBP2* can potentially predict the development of glaucoma. Consistent with the previous research, our findings suggest that LTBP2 mutations are associated with increased WTW measurements, indicating the presence of megalocornea [19, 42]. *ASPH* mutations are relatively rare, with only 19 cases reported until 2024 [35, 43]. Patients with *ASPH* mutations in this cohort exhibited distinct ocular features, including shortened AL, thinner corneal thickness, and reduced ACD. Chassaing et al. have shown that heterozygous mutations in *PTCH1* are deleterious, and ocular phenotypes such as microphthalmia, cataract, sclerosant cornea, anophthalmia, and anterior segment hypoplasia have been reported in patients carrying these mutations [44, 45].

We recognize that MSP often presents as a phenotype in other syndromes. Hence, these gene mutations can also cause systemic abnormalities. For example,

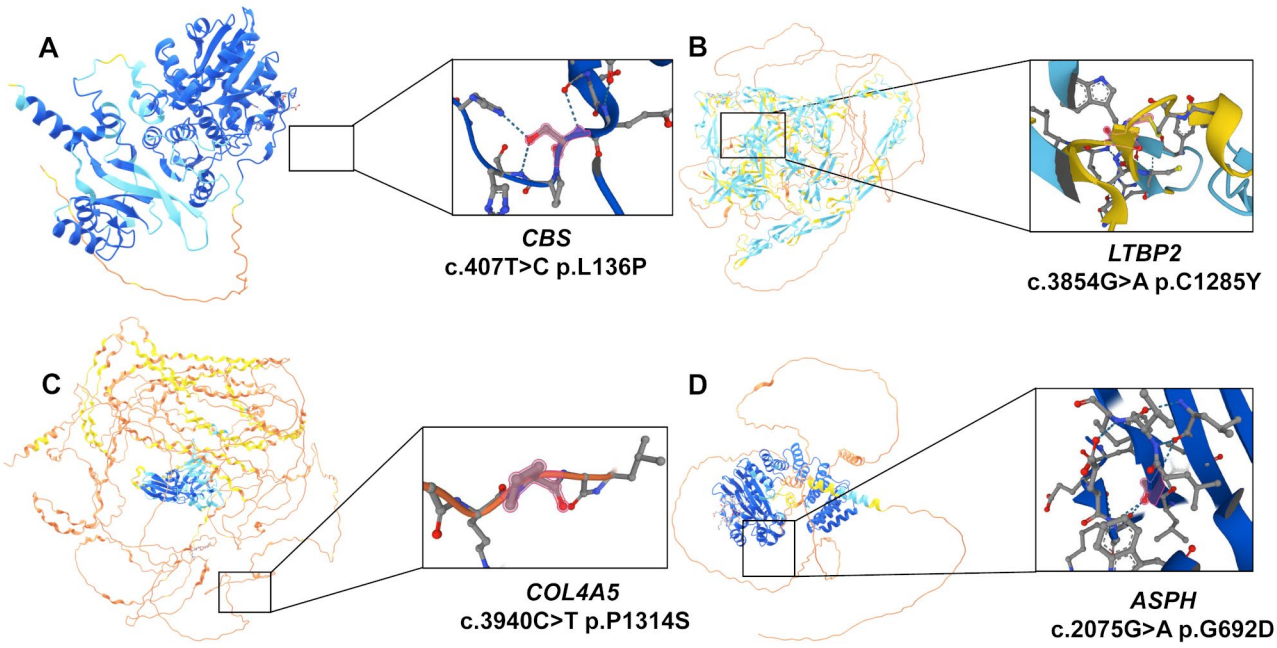

Fig. 3 Location and structural illustration of novel missense mutations in the 3D structure of the protein. (**A**) The *CBS* mutation (c.407T > C, p.L136P) and the inset provides a detailed view of the mutation site, highlighting the substitution at position 136 from the hydrophobic amino acid leucine to the hydrophilic, cyclic amino acid proline. (**B**) The *LTBP2* mutation (c.3854G > A, p.C1285Y), with the inset depicting the side-chain transition at position 1285 from the nonpolar cysteine to the polar tyrosine. (**C**) The *COL4A5* mutation (c.3940 C > T p.P1314S) and the inset is zoomed into the mutation site, demonstrating the exchange at position 1314 from the nonpolar amino acid proline to the polar amino acid serine. (**D**) The *ASPH* mutation (c.2075G > A p.G692D) and the inset is focused on the mutation site, showing the substitution at position 692 from the nonpolar glycine to the negatively charged, polar aspartic acid

LTBP2 and *ADAMTS17* commonly identified in patients with MWS patients. In this study, patients carrying *ADAMTS17* mutations were diagnosed at an older age and had a relatively longer lifespan [36]. Aside from genes associated with connective tissue, some pathogenic genes contributing to MSP are related to hereditary metabolic disorders, notably *CBS* and *SUOX*. These genes may promote the degradation of ciliary zonule by affecting disulfide bond function or increasing toxic metabolites in aqueous humor [12]. In this cohort, the severity of EL in patients with *CBS* mutations was second to those with *FBN1* mutations. The age at diagnosis for patients with *CBS* mutations was significantly earlier compared to others. Mulvihill et al. have indicated that ocular phenotypes in patients with *CBS* mutations typically manifest around the age of 3, with onset reported as early as 1 year and as late as 8 years [12]. *CBS* mutations weaken zonules and cause progressive EL [46]. Studies by Marjorie F. Lou et al. has shown that CBS protein levels in the anterior segment remains elevated throughout the lifespan [47]. Therefore, *CBS* mutations are also involve additional anterior segment abnormalities, potentially leading to iridodonesis, acute pupillary block, and even retinal detachment, optic nerve atrophy [12]. The difference is that most mutation sites in this cohort are located in the catalytic domain of *CBS*, rather than the Betaman module reported in other literatures [48]. This suggests that mutations in this region point to more pronounced ocular abnormalities.

The patient who carried a heterozygous missense mutation in *SUOX*, theoretically non-pathogenic, but this patient presented with binocular MSP and ametropia. Its pathogenesis needs further exploration. We hypothesize that if disease severity is related to a dose effect, preventive measures against serious neurologic complications become imperative.

In previous researches, mutations in *CNGB3* have been associated with functional impairment and degeneration of cone and rod cells [49, 50]. In our cohort, a novel *CNGB3* mutation combined with MSP was reported for the first time, yet its pathogenicity remains unclear. The *COL18A1* gene plays a major role in retinal structure and neural tube closure [51]. *COL4A5* mutations are implicated in Alport syndrome, with associated ocular manifestations including dot-and-fleck retinopathy, anterior cone of lens, and anterior polar cataract [52]. The type V collagen encoded by *COL5A2* regulates the growth of type I collagen fibers, and homozygous mutations in *COL5A2* have been demonstrated to cause skin and eye abnormalities in animal models. SLC16A12 is expressed in both retina and lens, and mutations in this gene have been associated with juvenile cataract, microcornea and

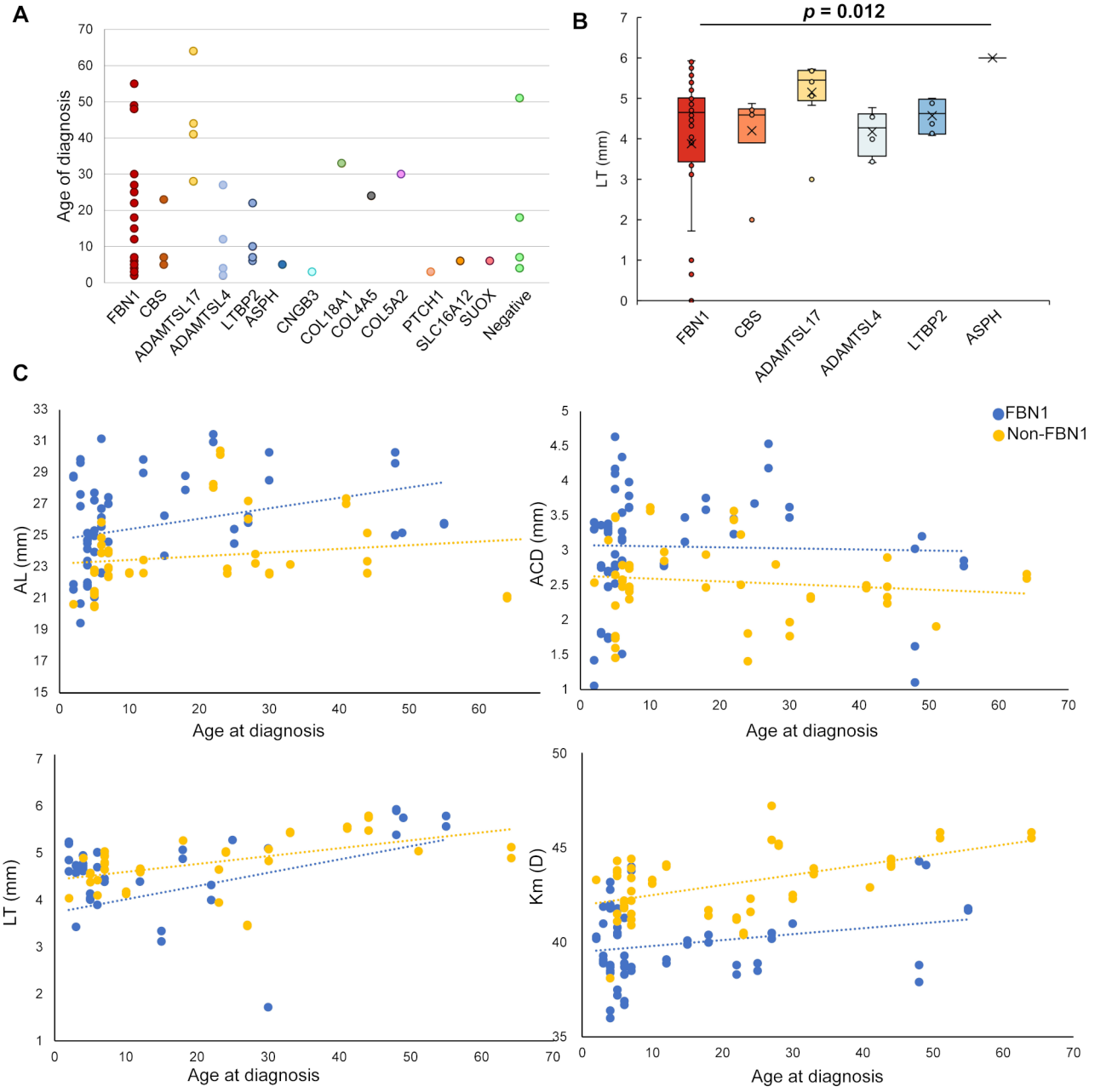

Fig. 4 Relationship between gene mutations, diagnostic age, and ocular biometric parameters. (**A**) Distribution of diagnostic ages among patients with 13 different gene mutations (*FBN1*, *CBS*, *ADAMTS17*, *ADAMTSL4*, *LTBP2*, *ASPH*, *CNGB3*, *COL18A1*, *COL4A5*, *COL5A2*, *PTCH1*, *SLC16A12*, *SUOX*, Negative) affecting MSP. (**B**) Boxplot illustrating LT among patients with six specific gene mutations (*FBN1*, *CBS*, *ADAMTS17*, *ADAMTSL4*, *LTBP2*, *ASPH*). (**C**) Variations in AL, ACD, LT, and Km with diagnostic age for individuals with *FBN1* mutations compared to non-*FBN1* mutations

glucosuria [53]. The early onset of these ocular manifestations implies that they might precede systemic complications, such as renal glucosuria, highlighting the need for timely monitoring of systemic manifestations [54].

In this study, the genetic mutations identified in MSP patients contribute to expanding the understanding of the genetic factors associated with the condition, offering potential insights that could guide future research into the genetic landscape of MSP. These findings notably improve diagnostic accuracy and efficiency, especially for patients exhibiting atypical clinical manifestations, where genetic-based precise diagnostics become increasingly feasible. Further analysis of the relationship between these new mutations and MSP phenotypes allows for a more accurate prediction of disease progression and severity, thereby providing patients with more precise prognostic information. Importantly, certain specific gene mutations may be closely associated with a higher

risk of complications, offering valuable guidance for the comprehensive management and monitoring strategies for MSP. Moreover, understanding how specific genetic mutations affect the clinical manifestations of MSP can aid physicians in developing more personalized treatment plans for patients.

However, we also acknowledge certain limitations within our study. Despite being one of the largest cohorts in existing MSP research, the sample size of 59 patients is still considered small within the field of genetic studies. This limits our ability to explore the association between some rare mutations and MSP. Additionally, the patient selection from specific regional medical institutions may introduce selection bias, suggesting that our findings could be limited to certain population characteristics and necessitate further validation across a broader demographic. Secondly, the high diversity between MSP phenotypes and genotypes adds complexity to the study. Different mutations within the same gene could lead to varied clinical presentations, necessitating cautious interpretation of the relationship between genetic variations and disease phenotypes. Furthermore, we did not engage in further mechanistic exploration. Future investigations will incorporate structural prediction and phenotypic validation studies to deepen our understanding.

Conclusion

In conclusion, the genetic background of MSP is very complex, and its pathogenic mechanism is also intricate. Comprehensive genetic landscape and phenotype studies play an important role in accurate diagnosis and mechanism research in MSP.

Supplementary Information

The online version contains supplementary material available at https://doi.org/10.1186/s40246-025-00729-6.

Supplementary Material 1

Acknowledgements
None.

Author contributions
Yan Liu: concept of paper, writing paper, data analysis. Yang Sun: data analysis; writing paper, data collection. Qiuyi Huo: data analysis; writing paper, data collection. Linghao Song: data collection. Xinyue Wang: data collection. Xin Shen: data collection. Ye Zhao: data collection. Tianhui Chen: data collection, critical review of the manuscript, data analysis. Yongxiang Jiang: study design, surgeon, critical review of the manuscript.

Funding
This study was supported by the National Natural Science Foundation of China (Grant no. 82070943), the National Natural Science Foundation of China (Grant no. 82271068), and Shanghai Science and Technology Commission (Grant no. 22Y11910400).

Data availability
No datasets were generated or analysed during the current study.

Declarations

Ethical approval and consent to participate
This study was approved by the institutional review board approved the study as an extension of our randomized controlled trial (ChiCTR2000039132). All patients had signed standard consent forms including consent for data privacy.

Consent for publication
Not applicable.

Competing interests
The authors have no conflicts of interest to disclose, and no propriety or commercial interest in any of the products discussed in this article.

Author details
[1]Eye Institute and Department of Ophthalmology, Eye & ENT Hospital, Fudan University, Shanghai 200031, China
[2]Key Laboratory of Myopia Key laboratory of Myopia and Related Eye Diseases, NHC; Key laboratory of Myopia and Related Eye Diseases, Chinese Academy of Medical Sciences, Shanghai 200031, China
[3]Shanghai Key Laboratory of Visual Impairment and Restoration, Shanghai 200031, China
[4]Department of Physiology and Pathophysiology, Shanghai Key Laboratory of Bioactive Small Molecules, School of Basic Medical Sciences, Fudan University, Shanghai 200031, China

Received: 3 May 2024 / Accepted: 13 February 2025
Published online: 01 March 2025

REFFERENCES

1. Yu X, Chen W, Xu W. Diagnosis and treatment of microspherophakia [J]. J Cataract Refract Surg. 2020;46(12):1674–9.
2. Khokhar S, Agarwal T, Kumar G, Kushmesh R. Tejwani L. K. Lenticular abnormalities in children [J]. J Pediatr Ophthalmol Strabismus. 2012;49(1):32–7.
3. Senthil S, Rao HL, Hoang NT, Jonnadula GB, Addepalli UK, Mandal AK, Garudadari CS. Glaucoma in microspherophakia: presenting features and treatment outcomes [J]. J Glaucoma. 2014;23(4):262–7.
4. Chen ZX, Chen TH, Zhang M, Chen JH, Lan LN, Deng M, Zheng JL, Jiang Y. X. correlation between FBN1 mutations and ocular features with ectopia lentis in the setting of Marfan syndrome and related fibrillinopathies [J]. Hum Mutat. 2021;42(12):1637–47.
5. Muralidhar R, Ankush K, Vijayalakshmi P. Visual outcome and incidence of glaucoma in patients with microspherophakia [J]. Eye (Lond). 2015;29(3):350–5.
6. Faivre L, Dollfus H, Lyonnet S, Alembik Y, Megarbane A, Samples J, Gorlin RJ, Alswaid A, Feingold J, Le Merrer M, Munnich A, Cormier-Daire V. Clinical homogeneity and genetic heterogeneity in Weill-Marchesani syndrome [J]. Am J Med Genet A. 2003;123A(2):204–7.
7. Greene VB, Stoetzel C, Pelletier V, Perdomo-Trujillo Y, Liebermann L, Marion V, De Korvin H, Boileau C, Dufier JL, Dollfus H. Confirmation of ADAMTSL4 mutations for autosomal recessive isolated bilateral ectopia lentis [J]. Ophthalmic Genet. 2010;31(1):47–51.
8. Guo D, Liu L, Yang F, Young CA, Zheng D, Jin G. Characteristics and genotype-phenotype correlations in ADAMTS17 mutation-related Weill-Marchesani syndrome [J]. Exp Eye Res. 2023;234:109606.
9. Xu M, Li K, He W. Compound heterozygous mutations in the LTBP2 gene associated with microspherophakia in a Chinese patient: a case report and literature review [J]. BMC Med Genomics. 2021;14(1):227.
10. Salchow Daniel J, Gehle, Petra. Ocular manifestations of Marfan syndrome in children and adolescents [J]. Eur J Ophthalmol. 2019;29(1):38–43.
11. Chen Zexu Z, Min D, Michael C, Tianhui C, Jiahui Z, Jialei J. Surgical outcomes of modified capsular tension ring and intraocular lens implantation in Marfan syndrome with ectopia lentis [J]. Eur J Ophthalmol. 2022;32(2):924–32.
12. Rahman M, Sharma M, Aggarwal P, Singla S, Jain N. Homocystinuria and ocular complications - a review [J]. Indian J Ophthalmol. 2022;70(7):2272–8.
13. Kumar A, Duvvari MR, Prabhakaran VC, Shetty JS, Murthy GJ, Blanton S. H. A homozygous mutation in LTBP2 causes isolated microspherophakia [J]. Hum Genet. 2010;128(4):365–71.

14. Zheng J, Cheng L, Chen Z, Chen T, Jiang Y. Factors Related to Visual Outcomes after Lens Surgery in Isolated Microspherophakia [J]. J Ophthalmol. 2022;2022:9089203.
15. Chen TH, Chen ZX, Zhang M, Chen JH, Deng M, Zheng JL, Lan LN, Jiang Y. X. Combination of panel-based next-generation sequencing and clinical findings in congenital ectopia lentis diagnosed in Chinese patients [J]. Am J Ophthalmol. 2022;237:278–98.
16. Chen ZX, Chen JH, Zhang M, Chen TH, Zheng JL, Deng M, Ji YH, Jiang Y. X. Analysis of Axial length in Young patients with Marfan syndrome and bilateral Ectopia Lentis by Z-Scores [J]. Ophthalmic Res. 2021;64(5):811–9.
17. Chan RT, Collin HB. Microspherophakia [J] Clin Exp Optom. 2002;85(5):294–9.
18. Chaudhary Sameer P, Manjur G, Niyatip V, Toshit K, Nareshb. Megalocornea and microspherophakia in homocysteinemia: a rare association [J]. Indian J Ophthalmol - Case Rep, 2023, 3(2).
19. Desir J, Sznajer Y, Depasse F, Roulez F, Schrooyen M, Meire F, Abramowicz M. LTBP2 null mutations in an autosomal recessive ocular syndrome with megalocornea, spherophakia, and secondary glaucoma [J]. Eur J Hum Genet. 2010;18(7):761–7.
20. Shreya TS, Senthilkumar VA, Mishra C, Krishnadas R. A rare presentation of bilateral dislocated lens in a patient with isolated microspherophakia [J]. Indian J Ophthalmol. 2020;68(6):1161–3.
21. Chen ZX, Jia WN, Jiang YX. Genotype-phenotype correlations of marfan syndrome and related fibrillinopathies: Phenomenon and molecular relevance. Front Genet. 2022;13:943083. https://doi.org/10.3389/fgene.2022.943083. Published 2022 Aug 16.
22. Chen Z, Chen T, Zhang M, Chen J, Deng M, Zheng J, Lan LN, Jiang Y. Fibrillin-1 gene mutations in a Chinese cohort with congenital ectopia lentis: spectrum and genotype-phenotype analysis [J]. Br J Ophthalmol. 2021;106(12):1655–61.
23. Putnam Elizabeth A, Mimi C, Arthur Z, Towbin Jeffrey B, Byers Peter A, Milewicz Dianna H. Delineation of the Marfan phenotype associated with mutations in exons 23–32 of theFBN1 gene [J]. Am J Med Genet. 1996;62(3):233–42.
24. Chen Z, Chen T, Zhang M, Chen J, Deng M, Zheng J, Lan LN, Jiang Y. Fibrillin-1 gene mutations in a Chinese cohort with congenital ectopia lentis: spectrum and genotype-phenotype analysis [J]. Br J Ophthalmol, 2021.
25. Guo D, Liu L, Ng KY, Cao Q, Zheng D, Zhang X, Jin G. Ocular, cardiovascular, and genetic characteristics and their associations in children with Marfan syndrome and related fibrillinopathies [J]. Graefes Arch Clin Exp Ophthalmol. 2023;261(11):3315–24.
26. Chen T, Chen Z, Du J, Zhang M, Chen Z, Gao Q, Chen A, Meng Q, Sun Y, Liu Y, Song L, Wang X, Edavi PP, Xu C, Zhang H, Huang J, Jiang Y. Reprogramming of iPSCs to NPCEC-like cells by biomimetic scaffolds for zonular fiber reconstruction [J]. Bioact Mater. 2025;45:446–58.
27. Inoue T, Ohbayashi T, Fujikawa Y, Yoshida H, Akama TO, Noda K, Horiguchi M, Kameyama K, Hata Y, Takahashi K, Kusumoto K, Nakamura T. Latent TGF-beta binding protein-2 is essential for the development of ciliary zonule microfibrils [J]. Hum Mol Genet. 2014;23(21):5672–82.
28. Shi Y, Jones W, Beatty W, Tan Q, Mecham RP, Kumra H, Reinhardt DP, Gibson MA, Reilly MA, Rodriguez J, Bassnett S. Latent-transforming growth factor beta-binding protein-2 (LTBP-2) is required for longevity but not for development of zonular fibers [J]. Matrix Biol. 2021;95:15–31.
29. Evans DR, Green JS, Fahiminiya S, Majewski J, Fernandez BA, Deardorff MA, Johnson GJ, Whelan JH, Hubmacher D. Care4rare Canada Consortium, Woods M. O. A novel pathogenic missense ADAMTS17 variant that impairs secretion causes Weill-Marchesani syndrome with variably dysmorphic hand features [J]. Sci Rep. 2020;10(1):10827.
30. Le Goff C, Cormier-Daire V. From tall to short: the role of TGFbeta signaling in growth and its disorders [J]. Am J Med Genet C Semin Med Genet. 2012;160 C(3):145–53.
31. Miao N, Zhang Y, Liao JY, Zhou L, He JC, Yang RQ, Liu XY, Tang L. Novel homozygous ADAMTS17 missense variant in Weill-Marchesani syndrome [J]. Int J Ophthalmol. 2023;16(5):694–9.
32. Dagoneau N, Benoist-Lasselin C, Huber C, et al. ADAMTS10 mutations in autosomal recessive Weill-Marchesani syndrome. Am J Hum Genet. 2004;75(5):801–6. https://doi.org/10.1086/425231
33. Karoulias SZ, Beyens A, Balic Z, Symoens S, Vandersteen A, Rideout AL, Dickinson J, Callewaert B. Hubmacher D. A novel ADAMTS17 variant that causes Weill-Marchesani syndrome 4 alters fibrillin-1 and collagen type I deposition in the extracellular matrix [J]. Matrix Biol. 2020;88:1–18.
34. Patel N, Khan AO, Mansour A, Mohamed JY, Al-Assiri A, Haddad R, Jia X, Xiong Y, Megarbane A, Traboulsi EI, Alkuraya FS. Mutations in ASPH cause facial dysmorphism, lens dislocation, anterior-segment abnormalities, and spontaneous filtering blebs, or Traboulsi syndrome [J]. Am J Hum Genet. 2014;94(5):755–9.
35. Lei C, Guo T, Ding S, Liao L, Peng H, Tan Z, Luo H. Whole-exome sequencing identified a novel homozygous ASPH frameshift variant causing Traboulsi syndrome in a Chinese family [J]. Mol Genet Genomic Med. 2021;9(1):e1553.
36. Huang J, Nie K, Lv X, Liu Y, Yang G, Fu J, Liu L, Lv H. Abnormal lens thickening in a child with Weill-Marchesani syndrome 4: a 3-year follow-up case report [J]. Front Med (Lausanne). 2022;9:1021489.
37. Chen ZX, Jia WN, Sun Y, et al. Biallelic ADAMTSL4 variants in a Chinese cohort of congenital ectopia lentis: implications for genotype-phenotype relationships. Hum Mutat. 2022;43(12):2141–52.
38. Aragon-Martin JA, Ahnood D, Charteris DG, Saggar A, Nischal KK, Comeglio P, Chandra A, Child AH, Arno G. Role of ADAMTSL4 mutations in FBN1 mutation-negative ectopia lentis patients [J]. Hum Mutat. 2010;31(8):E1622–31.
39. Knight LSW, Mullany S, Taranath DA, et al. The phenotypic spectrum of *ADAMTSL4*-associated ectopia lentis: Additional cases, complications, and review of literature. Mol Vis. 2022;28:257–68. Published 2022 Sep 4.
40. Le Goff C, Cormier-Daire V. The ADAMTS(L) family and human genetic disorders [J]. Hum Mol Genet. 2011;20(R2):R163–7.
41. Mead TJ, Apte SS. ADAMTS proteins in human disorders [J]. Matrix Biol. 2018;71–72:225– 39.
42. Morlino S, Alesi V, Cali F, Lepri FR, Secinaro A, Grammatico P, Novelli A, Drago F, Castori M, Baban A. LTBP2-related Marfan-like phenotype in two Roma/Gypsy subjects with the LTBP2 homozygous p.R299X variant [J]. Am J Med Genet A. 2019;179(1):104–12.
43. Chen ZX, Jia WN, Sun Y, Jiang YX. Genotype-phenotype profile of global ASPH-associated ectopia lentis and clinical findings from a Chinese cohort [J]. Gene. 2024;925:148600.
44. Black GC, Mazerolle CJ, Wang Y, Campsall KD, Petrin D, Leonard BC, Damji KF, Evans DG, Mcleod D. Wallace V. A. Abnormalities of the vitreoretinal interface caused by dysregulated hedgehog signaling during retinal development [J]. Hum Mol Genet. 2003;12(24):3269–76.
45. Chassaing N, Davis EE, Mcknight KL, Niederriter AR, Causse A, Desmaison DV, Lamarre A, Vincent-Delorme S, Pasquier C, Coubes L, Lacombe C, Rossi D, Dufier M, Dollfus JL, Kaplan H, Katsanis J, Etchevers N, Faguer HC, Calvas S. Targeted resequencing identifies PTCH1 as a major contributor to ocular developmental anomalies and extends the SOX2 regulatory network [J]. Genome Res. 2016;26(4):474–85.
46. Han Y, Shang Q, Yao J, Ji Y. Hydrogen sulfide: a gaseous signaling molecule modulates tissue homeostasis: implications in ophthalmic diseases [J]. Cell Death Dis. 2019;10(4):293.
47. Persa C, Osmotherly K, Chao-Wei Chen K, Moon S, Lou MF. The distribution of cystathionine beta-synthase (CBS) in the eye: implication of the presence of a trans-sulfuration pathway for oxidative stress defense [J]. Exp Eye Res. 2006;83(4):817–23.
48. Al-Sadeq DW, Nasrallah GK. The spectrum of mutations of Homocystinuria in the MENA region [J]. Genes (Basel), 2020, 11(3).
49. Ding XQ, Harry CS, Umino Y, Matveev AV, Fliesler SJ, Barlow RB. Impaired cone function and cone degeneration resulting from CNGB3 deficiency: down-regulation of CNGA3 biosynthesis as a potential mechanism [J]. Hum Mol Genet. 2009;18(24):4770–80.
50. Nishiguchi KM, Sandberg MA, Gorji N, Berson EL, Dryja TP. Cone cGMP-gated channel mutations and clinical findings in patients with achromatopsia, macular degeneration, and other hereditary cone diseases [J]. Hum Mutat. 2005;25(3):248–58.
51. Paisan-Ruiz C, Scopes G, Lee P, Houlden H. Homozygosity mapping through whole genome analysis identifies a COL18A1 mutation in an Indian family presenting with an autosomal recessive neurological disorder [J]. Am J Med Genet B Neuropsychiatr Genet. 2009;150B(7):993–7.
52. Kashtan CE. Alport syndrome. An inherited disorder of renal, ocular, and cochlear basement membranes. Med (Baltim). 1999;78(5):338–60. https://doi.org/10.1097/00005792-199909000-00005
53. Dhayat N, Simonin A, Anderegg M, Pathare G, Luscher BP, Deisl C, Albano G, Mordasini D, Hediger MA, Surbek DV, Vogt B, Sass JO, Kloeckener-Gruissem B. Fuster D. G. Mutation in the Monocarboxylate Transporter 12 Gene affects Guanidinoacetate Excretion but does not cause glucosuria [J]. J Am Soc Nephrol. 2016;27(5):1426–36.

54. Kloeckener-Gruissem B, Vandekerckhove K, Nurnberg G, Neidhardt J, Zeitz C, Nurnberg P, Schipper I, Berger W. Mutation of solute carrier SLC16A12 associates with a syndrome combining juvenile cataract with microcornea and renal glucosuria [J]. Am J Hum Genet. 2008;82(3):772–9.

Publisher's note